

# Uncovering the Limitations of Model Inversion Evaluation: Benchmarks and Connection to Type-I Adversarial Attacks

Sy-Tuyen Ho<sup>1\*</sup> Koh Jun Hao<sup>1\*</sup> Ngoc-Bao Nguyen<sup>1\*</sup>

Alexander Binder<sup>2</sup> Ngai-Man Cheung<sup>1</sup>

<sup>1</sup> Singapore University of Technology and Design (SUTD)

<sup>2</sup> Otto-von-Guericke University Magdeburg

sytuyen\_ho@mymail.sutd.edu.sg,

ngaiman\_cheung@sutd.edu.sg

## Abstract

*Model Inversion (MI) attacks aim to reconstruct information of private training data by exploiting access to machine learning models. The most common evaluation framework for MI attacks/defenses relies on an evaluation model that has been utilized to assess progress across almost all MI attacks and defenses proposed in recent years. In this paper, for the first time, we present an in-depth study of MI evaluation.*

*Firstly, we construct the first comprehensive human-annotated dataset of MI attack samples, based on 28 setups of different MI attacks, defenses, private and public datasets. Secondly, using our dataset, we examine the accuracy of the MI evaluation framework and reveal that it suffers from a significant number of false positives. These findings raise questions about the previously reported success rates of state-of-the-art (SOTA) MI attacks. Thirdly, we analyze the causes of these false positives, design controlled experiments, and discover the surprising effect of Type I adversarial features on MI evaluation, as well as adversarial transferability, highlighting a relationship between two previously distinct research areas. Our findings suggest that the performance of SOTA MI attacks has been overestimated, with the actual privacy leakage being significantly less than previously reported, e.g. the success rate of the latest SOTA attack, PLGMI [52], is 75.54% compared to the reported nearly 100%. In conclusion, we highlight critical limitations in the widely used MI evaluation framework and present our methods to mitigate false positive rates. We remark that prior research has shown that Type I adversarial attacks are very challenging [30, 45], with no existing solution. Therefore, we urge to consider human evaluation as a primary MI evaluation framework rather than merely a supplement as in previous MI research. We also encourage*

*further work on developing more robust and reliable automatic evaluation frameworks. Our dataset and code are available in the Supp.*

## 1. Introduction

Model Inversion (MI) attacks pose a significant privacy threat by attempting to reconstruct confidential information from sensitive training data through exploiting access to machine learning models. Recent state-of-the-art (SOTA) MI attacks [5, 31, 32, 35, 47, 52, 53] have shown considerable advancements, reporting attack success rates exceeding 90%. This vulnerability is particularly alarming for security-sensitive applications such as face recognition [13, 18, 27, 36], medical diagnosis [7, 8, 50], or speech recognition [4, 23].

**Research gap.** Recently, there are many studies on improving MI attacks [1, 5, 9, 14, 19, 31, 32, 35, 52, 53] and MI defenses [16, 22, 34, 42, 48]. To assess the effectiveness of these MI attacks/defenses, MI Attack Accuracy (AttAcc) is a standard and the most important metric. To measure MI AttAcc, almost all recent MI studies adopt the evaluation framework introduced by [53]. We denote this framework as  $\mathcal{F}_{Curr}$ . Under  $\mathcal{F}_{Curr}$ , an evaluation model  $E$ , distinct from the target model  $T$ , is used to predict the identities of individuals based on the MI reconstructed images as inputs.  $\mathcal{F}_{Curr}$  aims to automate MI evaluation and approximates manual evaluation by human. Particularly, let us consider the scenario where the adversary targets a specific identity  $y_{target}$ . The adversary produces reconstructed images  $x_{y_{target}}^{recon}$  of  $y_{target}$  by exploiting access to the target model  $T$ . To measure AttAcc, these  $x_{y_{target}}^{recon}$  samples are then passed through an evaluation model  $\hat{E}$  (distinct from  $T$ ). According to  $\mathcal{F}_{Curr}$ , the attack is deemed successful if  $E$  classifies  $x_{y_{target}}^{recon}$  as  $y_{target}$ . **Even though  $\mathcal{F}_{Curr}$  is used prevalently in almost all recent MI research and**

\*Equal Contribution

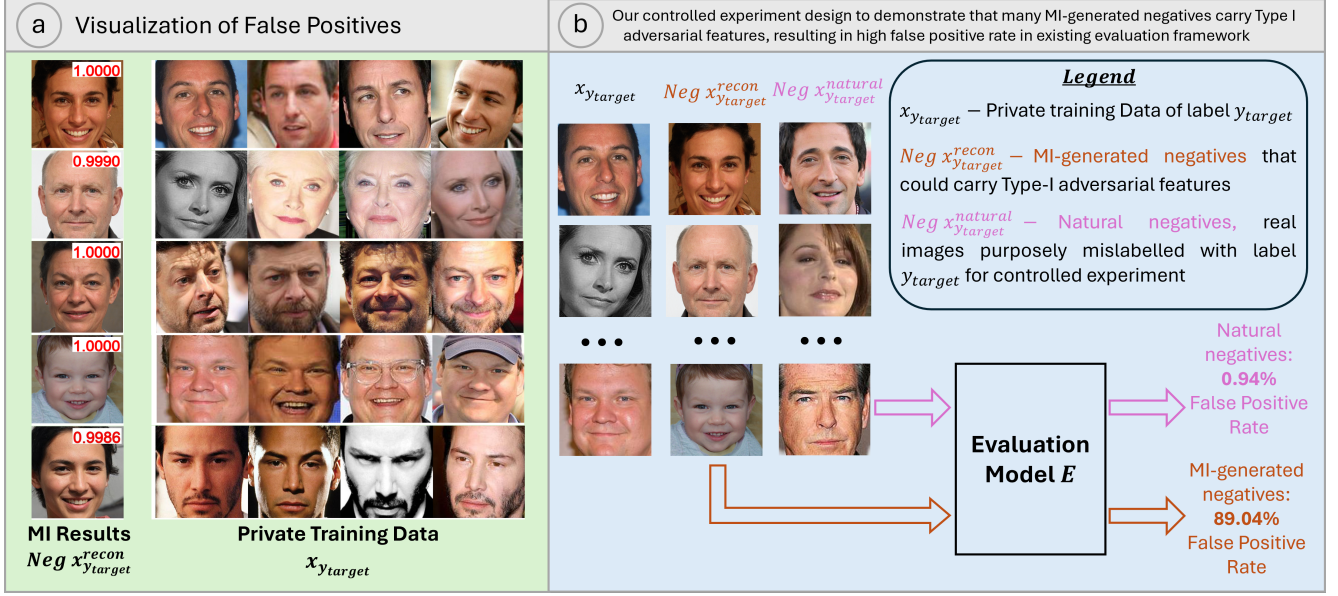


Figure 1. **In this work, we present the first and in-depth study on the Model Inversion (MI) evaluation.** Particularly, we investigate the most common MI evaluation framework  $\mathcal{F}_{Curr}$  to measure MI Attack Accuracy (AttAcc).  $\mathcal{F}_{Curr}$  is introduced in [53] and is utilized to assess almost all recent MI attacks/defenses. However, we find that  $\mathcal{F}_{Curr}$  suffers from a significant number of false positives. **(a) Visualization of False Positive (Comprehensive analysis in Sec. 3).** These false positive MI reconstructed samples do not capture visual identity features of the target individual in the private training data, but they are still deemed successful attacks according to  $\mathcal{F}_{Curr}$  with a high confidence (indicated in red text). Extensive visualization of false positives can be found in the Supp. **(b) Significant False Positives by  $\mathcal{F}_{Curr}$  are Type I Adversarial Examples (Comprehensive analysis in Sec. 4).** Our controlled experiment design to demonstrate that many MI-generated negatives carry Type I adversarial features, resulting in high false positive rate in existing evaluation framework.

the accuracy measured by  $\mathcal{F}_{Curr}$  has been the most important metric in gauging MI research progress, there has not been any in-depth and comprehensive study to understand the accuracy of  $\mathcal{F}_{Curr}$  and its limitations.

In this work, we conduct, for the first time, an in-depth study on the common MI evaluation framework  $\mathcal{F}_{Curr}$ . For an ideally successful attack, the reconstructed images  $x_{y_{target}}^{recon}$  should capture the visual identity features of  $y_{target}$ . However, we found that there exists a considerable number of MI reconstructed images that lack visual identity features of  $y_{target}$ , yet both target model  $T$  and evaluation model  $E$  under  $\mathcal{F}_{Curr}$  still assign high probabilities to  $y_{target}$ , i.e., high values of  $P_E(y_{target}|x_{y_{target}}^{recon})$ . Some examples are illustrated in Fig. 1-a. **These false positives potentially inflate the reported success rate of recent SOTA MI attacks.**

To carry out a rigorous study, we construct a comprehensive human-annotated dataset of MI attack samples. Using this dataset, we evaluate the accuracy of  $\mathcal{F}_{Curr}$  to measure MI AttAcc. Our study reveals that  $\mathcal{F}_{Curr}$  suffers from a significant number of false positives. The observed level of false positives raises questions about previously reported MI attack results. To shed light on the causes of these false positives, we systematically discover the effect of Type I

Adversarial Attacks [30, 45] on Model Inversion, highlighting a relationship between two previously distinct research areas. Importantly, the optimization processes in MI attacks and Type I adversarial attacks are similar: maximizing the likelihood with respect to (w.r.t.) input under a fixed model. Our findings demonstrate that significant false positives are Type I adversarial examples. Furthermore, due to the well-studied phenomenon *adversarial transferability* [30], these false positives can propagate to the MI evaluation model  $E$ , resulting in issue in  $\mathcal{F}_{Curr}$  and inflated success rates reported for recent MI attacks when using  $\mathcal{F}_{Curr}$ . To mitigate this issue, our initial efforts could reduce False Positive rates, however, they remains high. These results align with prior research on Type I Adversarial Attacks [30, 45], which highlights that Type I Adversarial Attacks are challenging with no existing solutions. Therefore, we urge human evaluation to be considered as a primary evaluation framework rather than merely a supplement to previous MI research. Additionally, we emphasize the need for increased research efforts toward developing more robust and reliable automatic MI evaluation frameworks.

We summarize our contributions as below:

- We present, for the first time, an in-depth study on the most common evaluation framework  $\mathcal{F}_{Curr}$  to compute

MI AttAcc.

- We construct a comprehensive human-annotated dataset of MI attack samples based on 28 setups of different MI attacks, defenses, private and public datasets, enabling us to assess the accuracy of  $\mathcal{F}_{Curr}$ . Our analysis reveals that  $\mathcal{F}_{Curr}$  suffers from a significant number of false positives. See Sec. 3.2.
- We discover, for the first time, the surprising effect of Type I Adversarial Features, as well as adversarial transferability [30, 45], on MI attacks, highlighting a relationship between two previously distinct research areas. Our findings explain numerous false positives in  $\mathcal{F}_{Curr}$ . (See Sec. 4.2)
- To mitigate this issue, we explore alternative evaluation frameworks (see Sec. 4.4). Although these approaches reduce false positive rates, they remain high, which is consistent with prior findings on Type I adversarial attacks [30, 45], with no existing effective solutions. We urge human evaluation to be considered as a primary MI evaluation framework rather than a supplement as in previous MI research.

## 2. Related Work

Model Inversion (MI) aims to extract information about the training data given a trained model. Particularly, an adversary exploits a target model  $T$  that was trained on a private dataset  $\mathcal{D}_{priv}$ . However,  $\mathcal{D}_{priv}$  should not be disclosed. The main goal of MI attacks is to extract information about the private samples in  $\mathcal{D}_{priv}$ . The existing literature formulates MI attacks as a process of reconstructing an input  $x_{target}^{recon}$  that  $T$  is likely to classify into the target class (label)  $y_{target}$ . For example, in facial recognition, MI attacks aim to reconstruct facial images that are likely to be identified as belonging to a particular person.

**Model Inversion Attack.** One of the initial methods for MI is proposed by Fredrikson et al. [9], who discover that attackers could use a machine learning model to extract genomic and demographic information about patients. Their work is extended to facial recognition [10], demonstrating the potential to reconstruct identifiable facial images from model outputs. Advancing this concept, Yang et al. [51] propose adversarial model inversion, treating the target model as an encoder and using a secondary network to reconstruct the original input data from the prediction vector. Recent advanced generative-based MI attack methods propose reducing the search space to the latent space by training a deep generator [5, 31, 35, 41, 47, 51–53], instead of directly performing MI attacks on high-dimensional space such as the image space. Specifically, GMI [53] and PPA [41] employ pretrained GAN models (e.g., WGAN [2] or StyleGAN [20]) on an auxiliary dataset similar to private training data  $\mathcal{D}_{priv}$ . Inversion images are found through the latent vector of the generator. Recent efforts have aimed

to enhance GAN-based MI methods from multiple perspectives. From the perspective of prior knowledge, KEDMI [5] proposes training inversion-specific GANs using knowledge from the target model  $T$ . Similarly, Pseudo-Label Guided MI [52] utilizes pseudo-labels to guide conditional GAN training, while IF-GMI [35] leverages intermediate feature representations from pretrained GAN blocks. From MI objective perspective, max-margin loss [52] and logit loss [31] are introduced to address limitations in Cross-Entropy loss used in MI attacks. From MI overfitting perspective, LOMMA [31] employs augmented model concepts to improve generalizability of MI attacks. The Eq. 1 represents the general step of existing SOTA MI attacks.

$$w^* = \arg \min_w (-\log P_T(y_{target}|G(w)) + \lambda \mathcal{L}_{prior}(w)) \quad (1)$$

Here,  $-\log P_T(y_{target}|G(w))$  represents the identity loss, guiding the reconstruction of  $x_{target}^{recon} = G(w)$  that is most likely to be classified as class  $y_{target}$  by target classifier  $T$ . The  $\mathcal{L}_{prior}$  is a prior loss, using public information to establish a distributional prior via GANs, thereby guiding the inversion process towards meaningful reconstructions.

**Model Inversion Defense.** In contrast to MI attacks, MI defenses aim to minimize the disclosure of training samples during the MI optimization process. To protect against MI attacks, the objective is to create a method to train the target classifier  $T$  on  $\mathcal{D}_{priv}$  in such a way that  $T$  reveals as little information about  $\mathcal{D}_{priv}$  as possible, regarding specific labels, while still achieving satisfactory model performance. Efforts have been made to develop defenses against MI attacks. MID [48] adds a regularizer to the target classifier’s objective during training, penalizing the mutual information between inputs  $x$  and outputs  $T(x)$ . BiDO [34] introduces a bilateral regularizer that minimizes the information about inputs  $x$  in feature representations  $z$  while maximizing the information about labels  $y$  in  $z$ . Beyond regularization-based defenses, TL-DMI [16] improves MI robustness through transfer learning, while LS [42] employs Negative Label Smoothing to improve MI robustness.

**Model Inversion Evaluation Metrics.** To evaluate MI attacks and defenses, almost all existing research primarily relies on the most common MI evaluation framework introduced in [53] to compute MI AttAcc. We denote this framework as  $\mathcal{F}_{Curr}$ . Let consider the scenario where the adversary targets a specific class  $y_{target}$ . The adversary generates reconstructed images  $x_{target}^{recon}$  by exploiting access to the target model  $T$ . These  $x_{target}^{recon}$  are then passed through an evaluation model  $E$  (distinct from  $T$ ). According to  $\mathcal{F}_{Curr}$ , the attack is deemed successful if  $E$  classifies  $x_{target}^{recon}$  as  $y_{target}$ . Other metrics such as KNN distance, FID, and Knowledge Extraction Score are also utilized by some studies. The KNN distance metric, used in [5, 16, 31, 41, 52, 53], measures the shortest feature dis-





Does Image A depict the same individual as the images in Set B?

Figure 2. **An example question of user studies for our human-annotated dataset of MI attack samples.** Our goal is to construct the ground truth label for MI reconstructed samples. We then use this dataset as a “gold standard” to assess the accuracy of MI evaluation framework. Particularly, the interface for each question in our user studies are illustrated as above. Here, an MI-reconstructed image  $x_{y_{target}}^{recon}$  of  $y_{target}$  is used as “Image A” while four real images of  $y_{target}$  are randomly selected as “Image B”. If participants respond “Yes”, the MI-reconstructed sample is labeled as a “Positive” sample (i.e., successful attack). Conversely, if participants respond “No”, it is labeled as a “Negative” sample (i.e., unsuccessful attack).

tance between the reconstructed image and actual images from the private dataset corresponding to the target class. Features for this comparison are extracted by the evaluation model  $E$  or an external feature extractor. FID is used in other works [34, 35, 41, 52] to assess the quality and realism of the reconstructions. Knowledge Extraction Score used in [42] measure the discriminative information extracted by an MI attack. Particularly, a surrogate classifier is trained on MI reconstructed images and measure its accuracy on the target model’s original training data. Despite some studies employing diverse metrics, the  $\mathcal{F}_{Curr}$  framework to compute MI AttAcc remains the most commonly used metric in almost MI attack and defense studies.

Even though  $\mathcal{F}_{Curr}$  is used prevalently in almost all recent MI research and the accuracy measured by  $\mathcal{F}_{Curr}$  has been the most important metric in gauging MI research progress, there has not been any in-depth and comprehensive study to understand the accuracy of  $\mathcal{F}_{Curr}$  and its limitations. In this work, we take the first step toward a comprehensive investigation of this MI evaluation framework.

### 3. Common Model Inversion (MI) Evaluation Framework $\mathcal{F}_{Curr}$ has issues

In this section, we present an in-depth investigation on prevalently used MI Evaluation Framework  $\mathcal{F}_{Curr}$  to compute MI AttAcc. First, to carry out a rigorous study, in Sec. 3.1, we construct a comprehensive human-annotated dataset of MI attack examples. Then, in Sec. 3.2, we use this dataset to evaluate the accuracy of  $\mathcal{F}_{Curr}$  to compute MI AttAcc, and reveal that it suffers from a significant number of false positives. Such significant level of false positives raises questions about previously reported MI attack results.

#### 3.1. Human-annotated dataset of MI attack samples

In this section, we present our comprehensive human-annotated dataset of MI attack samples. This dataset allows us to rigorously assess the accuracy of  $\mathcal{F}_{Curr}$ .

The primary aim of Model Inversion (MI) is to reconstruct images  $x_{y_{target}}^{recon}$  that closely resemble private training data  $x_{y_{target}} \sim \mathcal{D}_{priv}$ . Thus, for an ideally successful attack,  $x_{y_{target}}^{recon}$  should capture the visual identity features of  $y_{target}$ . Most, if not all, prevalent MI studies utilized common MI evaluation framework  $\mathcal{F}_{Curr}$  to compute MI AttAcc, which depends on the predictions of evaluation models  $E$  (distinct from target models  $T$ ). However, these evaluation models may have drawbacks related to overly stable predictions [30, 45]. To rigorously investigate this, we first establish a “gold standard” for evaluating MI attacks by constructing a human-annotated dataset of MI attack samples. Unlike a few existing human-involved studies in previous MI works [1, 16, 22, 31], our aim is to directly measure the true success rate of MI attacks rather than simply comparing the effectiveness of MI attacks or defenses.

**MI setups.** We use the prevalent MI setups from the literature to construct our dataset of MI attack samples. For each MI setup, we strictly follow the procedure in the previous MI studies. In total, our comprehensive dataset includes 28 standard and SOTA MI setups spanning 3 evaluation models  $E$ , 9 target classifiers  $T$ , 2 private datasets  $\mathcal{D}_{priv}$ , and 3 public datasets  $\mathcal{D}_{pub}$ . The detailed descriptions of the experimental setups are provided in the Supp.

**User Study Setup.** Our user study is implemented on Amazon Mechanical Turk (MTurk). Fig. 2 shows an example for our user studies. In our user study, participants are presented with a “Image A” and a set of “Image B” of a target class  $y_{target}$ , and then asked “Does Image A depict the same individual as the images in Set B?”. The answer to the question is binary, with options being either “Yes” or



MI Attack	$\mathcal{D}_{priv}$	$\mathcal{D}_{pub}$	$T$	$\mathcal{F}_{Human}$	$\mathcal{F}_{Curr}$					
				AttAcc $\uparrow$	$E$	AttAcc $\uparrow$	FP rate $\downarrow$	FN rate $\downarrow$	TP rate $\uparrow$	TN rate $\uparrow$
PPA [41]	FaceScrub [29]	FFHQ [20]	ResNet18 [15]	67.50%	InceptionNetV3 [44]	91.39%	89.04%	7.45%	92.52%	10.96%
			ResNet101 [15]	74.34%		84.69%	82.90%	14.69%	85.31%	17.10%
			ResNet152 [15]	75.36%		86.47%	85.87%	13.34%	86.66%	14.13%
			DenseNet121 [17]	73.52%		72.41%	66.52%	25.47%	74.53%	33.48%
			MaxViT [46]	70.80%		79.48%	76.17%	19.15%	80.85%	23.83%
IFGMI [35]	FaceScrub [29]	FFHQ [20]	ResNet18 [15]	76.88%	InceptionNetV3 [44]	95.62%	93.72%	3.81%	96.19%	6.28%
		MetFaces [21]	ResNet18 [15]	62.14%		72.13%	69.27%	26.13%	73.87%	30.73%
PLGMI [52]	CelebA [25]	CelebA [25]	VGG16 [39]	75.53%	FaceNet112 [6]	98.73%	97.55%	0.88%	99.12%	2.45%
		FFHQ [20]	VGG16 [39]	69.40%		88.67%	88.98%	11.91%	88.09%	10.02%
LOMMA [31]	CelebA [25]		IR152 [15]	78.82%	FaceNet112 [6]	92.02%	90.88%	7.70%	92.30%	9.12%
			CelebA [25]	FaceNet64 [6]		90.40%	91.69%	10.01%	89.99%	8.31%
			VGG16 [39]	72.40%		90.13%	89.13%	9.48%	90.52%	10.87%
			IR152 [15]	66.07%		77.74%	78.59%	22.70%	77.30%	21.41%
			FFHQ [20]	FaceNet64 [6]		72.13%	72.10%	27.85%	72.15%	27.90%
			VGG16 [39]	65.66%		63.07%	60.97%	35.84%	64.16%	39.03%
KEDMI [5]	CelebA [25]		IR152 [15]	73.93%	FaceNet112 [6]	79.27%	78.01%	20.29%	79.71%	21.99%
			CelebA [25]	FaceNet64 [6]		80.54%	78.02%	18.54%	81.46%	21.98%
			VGG16 [39]	77.87%		73.13%	70.78%	26.20%	73.80%	29.22%
			IR152 [15]	63.73%		52.20%	52.21%	47.80%	52.20%	47.79%
			FFHQ [20]	FaceNet64 [6]		54.60%	53.74%	44.94%	55.06%	46.26%
			VGG16 [39]	67.33%		42.47%	41.63%	57.13%	42.87%	58.37%

Table 1. **Our investigation on MI evaluation framework using our comprehensive dataset of MI attack samples.** Our investigation are based standard 28 MI setups focusing on SOTA and well established MI attacks/defense including PPA [41], LOMMA [35], KEDMI [5], PLGMI [52], IFGMI [35]. These 28 MI setups span 3 evaluation model  $E$ , 9 target classifier  $T$ , 2 private dataset  $\mathcal{D}_{priv}$ , 3 public dataset  $\mathcal{D}_{pub}$ . Detailed descriptions of the experimental setups are provided in the Supp. Overall, under  $\mathcal{F}_{Curr}$ , the results show that the number of false positives (FP) rates is significant. As a results, the threat of MI attacks has been overestimated in SOTA MI attacks, and the extent of leaked information is significantly less than previously assumed. E.g. SOTA MI attacks such as IFGMI [35], LOMMA [31], PLGMI [52], or PPA [41] claim over 90% to nearly 100% AttAcc in certain setups. However, the actual privacy leakage of these attacks remains below 80% across all setups.

“No”. The display order is randomized, with each image pair shown for a maximum of 60 seconds. There are total 400 participants each user study. We strictly follow MI setups from previous works [5, 16, 22, 31, 35, 41, 52] to generate MI reconstructed images. We strictly follow previous work on the number of questions (number of reconstructed images) and targeted classes. E.g., when  $\mathcal{D}_{priv} = \text{FaceScrub [29]}$ , there are total 4,240 questions encompassing all 530 target classes. When  $\mathcal{D}_{priv} = \text{CelebA [25]}$ , there are total 1,500 questions encompassing 300 target classes.

**Human-annotated dataset of MI attack samples.** We utilize the above user study setting to annotate the success rate of MI attack samples. Specifically, for each question, we select one MI-reconstructed image  $x_{y_{target}}^{recon}$  of  $y_{target}$  as “Image A” and randomly select 4 real images of  $y_{target}$  as “Image B”. If participants respond “Yes”,  $x_{y_{target}}^{recon}$  of  $y_{target}$  is labeled as a “Positive” sample (i.e., successful attack). Conversely, if participants respond “No”, it is labeled as a “Negative” sample (i.e., unsuccessful attack). For each setup, the number of “Yes” answers refer to the AttAcc via

human assessment. We denote the framework of user study to label/evaluate MI as  $\mathcal{F}_{Human}$ . This human-annotated dataset of MI attack samples serves as a “gold standard” for evaluate the accuracy of  $\mathcal{F}_{Curr}$  framework in Sec. 3.2. This dataset can also serve as ground truth for future studies on the MI evaluation framework.

### 3.2. What is the issue with the evaluation framework $\mathcal{F}_{Curr}$ for computing MI AttAcc?

In this section, using our human-annotated dataset of MI attack samples from Sec. 3.1, we demonstrate that using the common MI evaluation framework  $\mathcal{F}_{Curr}$  to compute MI AttAcc might have issues due to a significantly false-positive rates.

An ideally successful attack,  $x_{y_{target}}^{recon}$  should capture the visual identity of  $y_{target}$ . However, for a successful attack as according to  $\mathcal{F}_{Curr}$ ,  $x_{y_{target}}^{recon}$  only need to be classified as  $y_{target}$  by an evaluation model  $E$ . As shown in Fig. 1, we observe that within MI-reconstructed images  $x_{y_{target}}^{recon}$ , there are cases where the visual identity to  $y_{target}$  is minimal. Nevertheless,  $E$  assigns very high probabilities to  $y_{target}$  for these examples, i.e., high values of  $P_E(y_{target}|x_{y_{target}}^{recon})$ . We refer to these cases as false positives under the  $\mathcal{F}_{Curr}$  framework. When such false positives are numerous, they may inflate the reported success rates of MI attacks. To better understand the extent of this inflation, we compare the ground truth success rate (established in our constructed dataset in Sec. 3.1) to the success rate as measured by  $\mathcal{F}_{Curr}$  framework. Particularly, given the human-annotated labels in our dataset and the prediction via  $\mathcal{F}_{Curr}$ , we compute the False Positives (FP) rate, False Negatives (FN) rate, True Positives (TP) rate, and True Negatives (TN) rate for each MI setup. The AttAcc via  $\mathcal{F}_{Curr}$  is computed as:

$$\text{AttAcc}_{\mathcal{F}_{Curr}} = \frac{FP + TP}{FN + TP + FP + TN} \quad (2)$$

The results can be found in Tab. 1. We consistently observe that the FP rates are significant high across MI setups. In other words, there are numerous MI reconstructed images  $x_{y_{target}}^{recon}$  that do not capture visual identity of  $y_{target}$ , yet they are classified as  $y_{target}$  by the evaluation models  $E$ . Such high FP rate contributes to the significant inflation in reported AttAcc via  $\mathcal{F}_{Curr}$  of latest SOTA MI attack such as PPA [41], PLGMI [52], IFGMI [35], or LOMMA [31]. Notably, in their reported AttAcc using  $\mathcal{F}_{Curr}$ , these recent attacks report AttAcc values exceeding 90%, or even nearly 100% for certain setups. However, across a wide range of MI setups, the actual success rates never reach 80%. While we focus on high FP rates, FN rates also reveal limitations in the  $\mathcal{F}_{Curr}$ . Across MI setups, FN rates are consistently lower than FP rates. The FN rates depend on the classification accuracy and generalization capability of  $E$ . For example, under the PLGMI attack, when  $E = \text{FaceNet112}$

is trained on CelebA and evaluated with MI reconstructed images also from CelebA prior ( $\mathcal{D}_{pub} = \text{CelebA}$ ), FN rates are lower. In contrast, if this  $E$  is evaluated with MI reconstructed images from FFHQ prior ( $\mathcal{D}_{pub} = \text{FFHQ}$ ), FN rates increase due to distribution shifts.

Furthermore, in certain MI setups, we find that  $\mathcal{F}_{Curr}$  does not align well with  $\mathcal{F}_{Human}$  in evaluating MI attacks. For example, in the setup of MaxViT as  $T$  under the PPA attack, the AttAcc measured by  $\mathcal{F}_{Curr}$  is 11.91% lower than the setup for ResNet18 as  $T$  under the same attack. However, the MaxViT as  $T$  setup shows a 3.5% higher AttAcc measured by  $\mathcal{F}_{Human}$  than the ResNet18 as  $T$  setup. This suggests that, although less effective, the common MI evaluation framework  $\mathcal{F}_{Curr}$  could rate the attack as more successful than it actually is.

In conclusion, our analysis shows that **the common MI evaluation framework  $\mathcal{F}_{Curr}$  is suffered from very high FP rate, significantly affecting the reported results of contemporary MI studies based on  $\mathcal{F}_{Curr}$ .**

## 4. Significant False Positives by $\mathcal{F}_{Curr}$ are Type I Adversarial Examples

In this section, we explain the causes of these false positives. We discover, for the first time, the impact of Type I Adversarial Attack and MI Attacks, as well as adversarial transferability. Our analysis demonstrates that significant false positives as discussed are Type I Adversarial examples.

### 4.1. Adversarial Attack.

An adversarial attack on machine learning models is an intentional manipulation of input data to cause incorrect predictions, highlighting potential vulnerabilities of the model. Adversarial attacks aim to create inputs that deceive machine learning classifiers into making errors while humans do not. There are two main types of adversarial attacks: Type I and Type II. Type II Adversarial Attacks [3, 11, 24, 28, 33, 37, 43] are commonly studied and aim to produce false negatives. In this attack, minor and imperceptible perturbations are added to the input data  $x$  to generate an adversarial example  $x^{adv}$ , which is incorrectly classified by the model. Mathematically, this is represented as:

$$f(x^{adv}) \neq f(x) \text{ and } f_{human}(x^{adv}) = f_{human}(x) \quad (3)$$

Here,  $f$  is the model under attack,  $f_{human}$  is an oracle or a “ground truth” classifier, typically refer to human. In addition to Type II attack, Type I Adversarial Attacks are designed in [30, 45] to generate false positives by creating examples that are significantly different from the original input but are still classified as the same class by the model. This involves producing an adversarial example  $x^{adv}$  that,

despite being significantly different from input  $x$ , the model  $f$  mis-classifies as the original class. Mathematically, Type I adversarial attack sample is represented as [30, 45]:

$$f(x^{adv}) = f(x) \text{ and } f_{human}(x^{adv}) \neq f_{human}(x) \quad (4)$$

One way to produce Type I adversarial examples involves optimizing the input by iteratively updating it to maximize the likelihood under a fixed target model classifier [30]. This process optimizes the input to remain within a targeted decision boundary, however, it is different from training data by human perception. This phenomenon can also be viewed as over-confidence phenomenon of machine learning models [12, 49].

#### 4.2. The effect of Type I adversarial features on MI in producing false positives.

Due to the similarity nature of Type I adversarial attacks and MI, i.e. maximizing the likelihood with respect to (w.r.t) input under a fixed model, we hypothesize that a significant number of MI reconstructed samples  $x_{y_{target}}^{recon}$  carrying Type I adversarial features. As a result, they are mis-classified by  $T$  and  $E$  into  $y_{target}$  although these  $x_{y_{target}}^{recon}$  do not resemble  $x_{y_{target}}$  (Eq. 6). We conduct experiments to validate our hypothesis. We take the two MI setups: • Setup 1:  $T$ = ResNet18,  $\mathcal{D}_{priv}$ = FaceScrub, attack = PPA,  $E$ = InceptionV3/ MaxViT • Setup 2:  $T$ = VGG16,  $\mathcal{D}_{priv}$ = CelebA, attack = PLGMI,  $E$ = FaceNet112. We conduct this experiment on a comprehensive setting with all evaluation models  $E$  used in previous MI studies (i.e., InceptionNetV3 for PPA on and FaceNet112 for PLGMI) and an additional architecture of  $E$  (i.e., MaxViT for PPA). We first perform MI attacks to obtain MI-generated samples  $x_{y_{target}}^{recon}$ . We then identified all **MI-generated negative samples**, denoted as Neg  $x_{y_{target}}^{recon}$ , through human annotation ( $f_{human}(\text{Neg } x_{y_{target}}^{recon}) \neq f_{human}(x_{y_{target}})$ ). Let  $n$  denote the number of MI-generated negative samples ( $|\text{Neg } x_{y_{target}}^{recon}| = n$ ). We create another dataset of **natural negative samples**, denoted as Neg  $x_{y_{target}}^{natural}$ , which is free from Type I adversarial attack, for controlled experiments. We do so by randomly selecting  $n$  FFHQ images (no class overlapping with FaceScrub), and intentionally mis-label these FFHQ images with randomly selected FaceScrub identities, obtaining  $n$  Neg  $x_{y_{target}}^{natural}$  ( $f_{human}(\text{Neg } x_{y_{target}}^{natural}) \neq f_{human}(x_{y_{target}})$ ). Importantly, unlike Neg  $x_{y_{target}}^{recon}$ , these Neg  $x_{y_{target}}^{natural}$  are randomly selected from FFHQ and therefore they are free from Type I adversarial attack. Neg  $x_{y_{target}}^{natural}$  is our controlled dataset.

We pass Neg  $x_{y_{target}}^{recon}$  and Neg  $x_{y_{target}}^{natural}$  into  $E$ , and count the number of false positive, i.e., Neg  $x_{y_{target}}^{recon}$  / Neg  $x_{y_{target}}^{natural}$  being mis-classified into  $y_{target}$ . Our experimental setup are illustrated in Fig. 1-b and the false positive rate of Neg  $x_{y_{target}}^{recon}$  and Neg  $x_{y_{target}}^{natural}$  are compared in Tab. 2. MI-generated negatives Neg  $x_{y_{target}}^{recon}$ , with Type I adversarial

feature learned during MI, have a high FP rate, whereas natural negatives Neg  $x_{y_{target}}^{natural}$ , which are free from Type I adversarial feature, have a low FP rate. For example, in Setup 1, FP rates of Neg  $x_{y_{target}}^{recon}$  is 89.04% while FP rates of Neg  $x_{y_{target}}^{natural}$  is 0.94%. This experiment further demonstrates the effect of Type I Adversarial features in MI evaluation resulting in a significant number of false positives.

Attack	$\mathcal{D}_{priv}$	$E$	FP rates under $E$	
PPA	FaceScrub	InceptionV3	Neg $x_{y_{target}}^{recon}$	89.04%
			Neg $x_{y_{target}}^{natural}$	0.94%
		MaxViT	Neg $x_{y_{target}}^{recon}$	73.95%
			Neg $x_{y_{target}}^{natural}$	0.22%
PLGMI	CelebA	FaceNet112	Neg $x_{y_{target}}^{recon}$	97.55%
			Neg $x_{y_{target}}^{natural}$	0.00%

Table 2. **Our controlled experiment to show the effect of Type I adversarial attacks in MI on false positive rates.** We compare false positive rate of negative  $x_{y_{target}}^{recon}$  and negative  $x_{y_{target}}^{natural}$ . Many  $x_{y_{target}}^{recon}$  are affected by Type I adversarial attack during MI, whereas Neg  $x_{y_{target}}^{natural}$  is free from Type I adversarial feature (see main text for creation of Neg  $x_{y_{target}}^{natural}$ ). Due to Type I adversarial attack,  $x_{y_{target}}^{recon}$  has a significantly high false positive rate. We conduct this experiment on a comprehensive setting with all evaluation models  $E$  used in previous MI studies (i.e., InceptionNetV3 for PPA on and FaceNet112 for PLGMI) and an additional architecture of  $E$  (i.e., MaxViT for PPA)

	False Positive in MI	Type I Adversarial Attack
Fixed Model Under Attack	$T$	$f$
Private/Original Sample	$x_{y_{target}}$	$x$
Attack Sample	$x_{y_{target}}^{recon}$	$x^{adv}$
Formulation	$T(x_{y_{target}}^{recon}) = T(x_{y_{target}})$	$f(x^{adv}) = f(x)$
	$f_{human}(x_{y_{target}}^{recon}) \neq f_{human}(x_{y_{target}})$	$f_{human}(x^{adv}) \neq f_{human}(x)$

Table 3. Connection between False Positive (FP) in MI (Eq. 5) and Type I adversarial attack (Eq. 4) [30, 45].

#### 4.3. MI Attacks and Type I Adversarial Attacks.

The results in Sec. 4.2 demonstrate the impact of Type I Adversarial Attacks on MI attacks results. In what follows, we further discuss this impact through a systematic analysis between false positives in MI attacks Type I adversarial attacks. Importantly, both MI and adversarial attacks exploit a fixed target model by maximizing the likelihood under the fixed target model w.r.t. the input, see Tab. 3.

Mathematically, false positives in MI can be interpreted



similarly to Type I adversarial attack samples as represented in Eq. 4. Specifically, with target classifier  $T$  and  $f_{human}$  denoting the oracle (e.g. human), false positive in MI attack is represented as:

$$\begin{aligned} T(x_{y_{target}}^{recon}) &= T(x_{y_{target}}) = y_{target} \\ \text{and } f_{human}(x_{y_{target}}^{recon}) &\neq f_{human}(x_{y_{target}}) \end{aligned} \quad (5)$$

Here,  $x_{y_{target}}^{recon}$  does not resemble the visual identity feature of  $x_{y_{target}}$ . However,  $T$  classifies  $x_{y_{target}}^{recon}$  as  $y_{target}$ . Hence,  $x_{y_{target}}^{recon}$  is a false positive in MI. By comparing Eq. 5 and Eq. 4, the link between false positives in MI and Type I adversarial can be noted, with the correspondences listed in Tab. 3.

In Eq. 5, an alternative interpretation is that the false positive  $x_{y_{target}}^{recon}$  is the example that can deceive  $T$  to classify it as  $y_{target}$  while human can not recognize  $x_{y_{target}}^{recon}$  as  $y_{target}$ . Moreover, due to the transferability of Type I adversarial attack [30], these false positives can propagate to MI evaluation model  $E$  expressed mathematically as:

$$\begin{aligned} E(x_{y_{target}}^{recon}) &= E(x_{y_{target}}) = y_{target} \\ \text{and } f_{human}(x_{y_{target}}^{recon}) &\neq f_{human}(x_{y_{target}}) \end{aligned} \quad (6)$$

Overall, Type I adversarial attack affects MI attack on  $T$  and evaluation based on  $E$ , giving rise to a significant number of false positives in  $\mathcal{F}_{Curr}$ .

#### 4.4. Our efforts to mitigate the impact of Type I Adversarial Attacks on MI Evaluation

Our study so far suggests that the prevalently used MI evaluation framework  $\mathcal{F}_{Curr}$  may be ineffective and unreliable in accurately evaluating MI attacks. Our investigation strictly follows  $\mathcal{F}_{Curr}$  as used in previous MI studies [5, 31, 35, 41, 52]. In this section, we further present our efforts to mitigate the impact of Type I Adversarial Attacks on  $\mathcal{F}_{Curr}$ . Particularly, we explore three alternative MI evaluation frameworks:  $\mathcal{F}_{MaxViT}$ ,  $\mathcal{F}_{Adv}$ , and  $\mathcal{F}_{Ens}$ .

For  $\mathcal{F}_{MaxViT}$ , we utilize MaxViT [46] as an Evaluation Model  $E$ . Vision Transformer based architectures have demonstrated to be more robust than CNNs counterparts [38]. Furthermore, transferring adversarial examples across ViTs and CNNs is even more difficult because their structures and image-processing mechanisms are fundamentally different [26].

For  $\mathcal{F}_{Adv}$ , we utilize an adversarially trained Evaluation Model  $E$  with the same architecture as in the original setup. Similarly to  $\mathcal{F}_{MaxViT}$ , adversarial training has been shown to improve adversarial robustness in the literature. We adopt adversarial training setups from [40] using 2-step APGD with a  $\ell_\infty$  radius of 2/255.

For  $\mathcal{F}_{Ens}$ , we employ an ensemble of three Evaluation Model  $E$  for the MI evaluation. Ensemble models are known to reduce adversarial transferability. Unlike

$\mathcal{F}_{Human}$	MI Evaluation		FP rate
AttAcc	Framework		
67.50%	$\mathcal{F}_{Curr}$	91.39%	89.04%
	$\mathcal{F}_{MaxViT}$	79.36%	73.95%
	$\mathcal{F}_{Adv}$	68.35%	63.06%
	$\mathcal{F}_{Ens}$	75.59%	71.69%

Table 4. We explore approaches such as  $\mathcal{F}_{MaxViT}$  (utilizing MaxViT architecture for the evaluation model),  $\mathcal{F}_{Adv}$  (utilizing adversarially trained evaluation model), and  $\mathcal{F}_{Ens}$  (utilizing multiple evaluation models for ensemble evaluation) aiming to reduce the effect of Type I Adversarial Attack to MI evaluation. The results confirm false positives are reduced, but there is room for improvement. This aligns with the literature on Type I Adversarial Attack, which highlights the lack of effective defenses [30, 45]. Therefore, we urge to consider human evaluation as a primary MI framework and encourage research into more robust automatic evaluation methods.

$\mathcal{F}_{MaxViT}$  and  $\mathcal{F}_{Adv}$  aiming to improve the robustness of  $E$ ,  $\mathcal{F}_{Ens}$  focuses on mitigating adversarial transferability, potentially lowering false positive rates by avoiding relying only on a single  $E$ . For implementation, we strictly reuse the training code of  $E$  with the same architecture and training method as the original setup.

Here, we focus on high-resolution setups of PPA attacks, with ResNet18 as  $T$ , FaceScrub as  $\mathcal{D}_{priv}$ , and FFHQ as  $\mathcal{D}_{pub}$ . For a fair comparison, we follow the original training procedure of  $E$  and ensure that its model utility remains comparable across all MI evaluation frameworks.

The results can be found in Tab. 4. We observe that while false positives are reduced, they remain significantly high. Our results reinforce existing literature on Type I Adversarial Attack [30, 45] highlighting that Type I Adversarial Attack is challenging with no effective solution. Therefore, we urge to consider human evaluation as a primary MI evaluation framework rather than merely a supplement as in previous MI research. We also encourage further work on developing more robust and reliable automatic evaluation frameworks. We also encourage further work on developing more robust and reliable automatic evaluation frameworks.

## 5. Conclusion

In this work, we present the first in-depth study of MI evaluation. We construct a comprehensive human-annotated dataset of MI attack samples, spanning 28 common MI setups, to assess the reliability of the widely used MI evaluation framework. Our findings reveal critical limitations, particularly due to high false positive rates that have led to overestimated success rates of SOTA MI attacks. Furthermore, we designed a controlled experiment to demonstrate

that many negative examples generated from MI are Type-I adversarial examples, contributing to false positives in the current evaluation framework. We proposed improved solution, and remark that prior research has shown that Type I adversarial attacks are very challenging [30, 45], with no existing solution. Therefore, we urge to consider human evaluation as a primary MI evaluation framework rather than merely a supplement as in previous MI research. Supported by our proposed dataset, we further encourage the development of more reliable automatic evaluation frameworks. **Our code, dataset and additional results are in Supp.**

## References

- [1] Shengwei An, Guanhong Tao, Qiuling Xu, Yingqi Liu, Guangyu Shen, Yuan Yao, Jingwei Xu, and Xiangyu Zhang. Mirror: Model inversion for deep learning network with high fidelity. In *Proceedings of the 29th Network and Distributed System Security Symposium*, 2022. 1, 4
- [2] Martin Arjovsky, Soumith Chintala, and Léon Bottou. Wasserstein generative adversarial networks. In *International conference on machine learning*, pages 214–223. PMLR, 2017. 3
- [3] Nicholas Carlini and David Wagner. Towards evaluating the robustness of neural networks. In *2017 IEEE Symposium on Security and Privacy (SP)*, pages 39–57. Ieee, 2017. 6
- [4] Xuankai Chang, Wangyou Zhang, Yanmin Qian, Jonathan Le Roux, and Shinji Watanabe. End-to-end multi-speaker speech recognition with transformer. In *ICASSP 2020*, pages 6134–6138. IEEE, 2020. 1
- [5] Si Chen, Mostafa Kahla, Ruoxi Jia, and Guo-Jun Qi. Knowledge-enriched distributional model inversion attacks. In *Proceedings of the IEEE/CVF international conference on computer vision*, pages 16178–16187, 2021. 1, 3, 5, 8, 13, 16, 17
- [6] Yu Cheng, Jian Zhao, Zhecan Wang, Yan Xu, Karlekar Jayashree, Shengmei Shen, and Jiashi Feng. Know you at one glance: A compact vector representation for low-shot learning. In *Proceedings of the IEEE ICCV Workshops*, pages 1924–1932, 2017. 5
- [7] Jonas Dippel, Steffen Vogler, and Johannes Höhne. Towards fine-grained visual representations by combining contrastive learning with image reconstruction and attention-weighted pooling. *arXiv preprint arXiv:2104.04323*, 2021. 1
- [8] Benoit Dufumier, Pietro Gori, Julie Victor, Antoine Grigis, Michele Wessa, Paolo Brambilla, Pauline Favre, Mircea Polosan, Colm McDonald, Camille Marie Pigué, et al. Contrastive learning with continuous proxy meta-data for 3d mri classification. In *MICCAI 2021*. Springer, 2021. 1
- [9] Matthew Fredrikson, Eric Lantz, Somesh Jha, Simon Lin, David Page, and Thomas Ristenpart. Privacy in pharmacogenetics: An end-to-end case study of personalized warfarin dosing. In *23rd USENIX Security Symposium (USENIX Security 14)*, pages 17–32, 2014. 1, 3
- [10] Matt Fredrikson, Somesh Jha, and Thomas Ristenpart. Model inversion attacks that exploit confidence information and basic countermeasures. In *Proceedings of the 22nd ACM SIGSAC conference on computer and communications security*, pages 1322–1333, 2015. 3
- [11] Ian J Goodfellow, Jonathon Shlens, and Christian Szegedy. Explaining and harnessing adversarial examples. *arXiv preprint arXiv:1412.6572*, 2014. 6
- [12] Chuan Guo, Geoff Pleiss, Yu Sun, and Kilian Q Weinberger. On calibration of modern neural networks. In *ICML*, pages 1321–1330. PMLR, 2017. 7
- [13] Jianzhu Guo, Xiangyu Zhu, Chenxu Zhao, Dong Cao, Zhen Lei, and Stan Z Li. Learning meta face recognition in unseen domains. In *CVPR*, pages 6163–6172, 2020. 1
- [14] Gyojin Han, Jaehyun Choi, Haeil Lee, and Junmo Kim. Reinforcement learning-based black-box model inversion attacks. In *CVPR*, pages 20504–20513, 2023. 1
- [15] Kaiming He, Xiangyu Zhang, Shaoqing Ren, and Jian Sun. Deep residual learning for image recognition. In *Proceedings of the IEEE conference on computer vision and pattern recognition*, pages 770–778, 2016. 5, 12, 13, 14, 15, 16, 17
- [16] Sy-Tuyen Ho, Koh Jun Hao, Keshigeyan Chandrasegaran, Ngoc-Bao Nguyen, and Ngai-Man Cheung. Model inversion robustness: Can transfer learning help? In *Proceedings of the IEEE/CVF Conference on Computer Vision and Pattern Recognition*, pages 12183–12193, 2024. 1, 3, 4, 5, 12, 13, 16, 17
- [17] Gao Huang, Zhuang Liu, Laurens Van Der Maaten, and Kilian Q Weinberger. Densely connected convolutional networks. In *Proceedings of the IEEE conference on computer vision and pattern recognition*, pages 4700–4708, 2017. 5, 12, 17
- [18] Yuge Huang, Yuhan Wang, Ying Tai, Xiaoming Liu, Pengcheng Shen, Shaoxin Li, Jilin Li, and Feiyue Huang. Curricularface: adaptive curriculum learning loss for deep face recognition. In *proceedings of the IEEE/CVF conference on computer vision and pattern recognition*, pages 5901–5910, 2020. 1
- [19] Mostafa Kahla, Si Chen, Hoang Anh Just, and Ruoxi Jia. Label-only model inversion attacks via boundary repulsion. In *Proceedings of the IEEE/CVF Conference on Computer Vision and Pattern Recognition*, pages 15045–15053, 2022. 1
- [20] Tero Karras, Samuli Laine, and Timo Aila. A style-based generator architecture for generative adversarial networks. In *Proceedings of the IEEE/CVF conference on computer vision and pattern recognition*, pages 4401–4410, 2019. 3, 5, 12, 13, 14, 15, 16, 17
- [21] Tero Karras, Miika Aittala, Janne Hellsten, Samuli Laine, Jaakko Lehtinen, and Timo Aila. Training generative adversarial networks with limited data. *Advances in neural information processing systems*, 33:12104–12114, 2020. 5, 12
- [22] Jun Hao Koh, Sy-Tuyen Ho, Ngoc-Bao Nguyen, and Ngai-man Cheung. On the vulnerability of skip connections to model inversion attacks. *arXiv preprint arXiv:2409.01696*, 2024. 1, 4, 5, 12, 13, 16, 17
- [23] Gautam Krishna, Co Tran, Jianguo Yu, and Ahmed H Tewfik. Speech recognition with no speech or with noisy speech. In *ICASSP 2019-2019 IEEE International Conference on*

- Acoustics, Speech and Signal Processing (ICASSP)*, pages 1090–1094. IEEE, 2019. 1
- [24] Alexey Kurakin, Ian Goodfellow, and Samy Bengio. Adversarial machine learning at scale. *arXiv preprint arXiv:1611.01236*, 2016. 6
- [25] Ziwei Liu, Ping Luo, Xiaogang Wang, and Xiaoou Tang. Deep learning face attributes in the wild. In *Proceedings of the IEEE international conference on computer vision*, pages 3730–3738, 2015. 5, 16, 17
- [26] Wenshuo Ma, Yidong Li, Xiaofeng Jia, and Wei Xu. Transferable adversarial attack for both vision transformers and convolutional networks via momentum integrated gradients. In *Proceedings of the IEEE/CVF International Conference on Computer Vision*, pages 4630–4639, 2023. 8, 11
- [27] Qiang Meng, Shichao Zhao, Zhida Huang, and Feng Zhou. Magface: A universal representation for face recognition and quality assessment. In *Proceedings of the IEEE/CVF Conference on Computer Vision and Pattern Recognition*, pages 14225–14234, 2021. 1
- [28] Seyed-Mohsen Moosavi-Dezfooli, Alhussein Fawzi, and Pascal Frossard. Deepfool: a simple and accurate method to fool deep neural networks. In *Proceedings of the IEEE conference on computer vision and pattern recognition*, pages 2574–2582, 2016. 6
- [29] Hong-Wei Ng and Stefan Winkler. A data-driven approach to cleaning large face datasets. In *2014 IEEE international conference on image processing (ICIP)*, pages 343–347. IEEE, 2014. 5, 12, 13, 14, 15, 16
- [30] Anh Nguyen, Jason Yosinski, and Jeff Clune. Deep neural networks are easily fooled: High confidence predictions for unrecognizable images. In *Proceedings of the IEEE conference on computer vision and pattern recognition*, pages 427–436, 2015. 1, 2, 3, 4, 6, 7, 8, 9
- [31] Ngoc-Bao Nguyen, Keshigeyan Chandrasegaran, Milad Abdollahzadeh, and Ngai-Man Cheung. Re-thinking model inversion attacks against deep neural networks. In *Proceedings of the IEEE/CVF Conference on Computer Vision and Pattern Recognition (CVPR)*, 2023. 1, 3, 4, 5, 6, 8, 13, 16, 17
- [32] Ngoc-Bao Nguyen, Keshigeyan Chandrasegaran, Milad Abdollahzadeh, and Ngai man Cheung. Label-only model inversion attacks via knowledge transfer. In *Thirty-seventh Conference on Neural Information Processing Systems*, 2023. 1
- [33] Nicolas Papernot, Patrick McDaniel, Somesh Jha, Matt Fredrikson, Z Berkay Celik, and Ananthram Swami. The limitations of deep learning in adversarial settings. In *2016 IEEE European symposium on security and privacy (EuroS&P)*, pages 372–387. IEEE, 2016. 6
- [34] Xiong Peng, Feng Liu, Jingfeng Zhang, Long Lan, Junjie Ye, Tongliang Liu, and Bo Han. Bilateral dependency optimization: Defending against model-inversion attacks. In *KDD*, 2022. 1, 3, 4
- [35] Yixiang Qiu, Hao Fang, Hongyao Yu, Bin Chen, MeiKang Qiu, and Shu-Tao Xia. A closer look at gan priors: Exploiting intermediate features for enhanced model inversion attacks. *arXiv preprint arXiv:2407.13863*, 2024. 1, 3, 4, 5, 6, 8, 12, 13, 15, 16, 17
- [36] Florian Schroff, Dmitry Kalenichenko, and James Philbin. Facenet: A unified embedding for face recognition and clustering. In *Proceedings of the IEEE conference on computer vision and pattern recognition*, pages 815–823, 2015. 1
- [37] Ali Shafahi, Mahyar Najibi, Mohammad Amin Ghiasi, Zheng Xu, John Dickerson, Christoph Studer, Larry S Davis, Gavin Taylor, and Tom Goldstein. Adversarial training for free! *Advances in neural information processing systems*, 32, 2019. 6
- [38] Rulin Shao, Zhouxing Shi, Jinfeng Yi, Pin-Yu Chen, and Cho-Jui Hsieh. On the adversarial robustness of vision transformers. *arXiv preprint arXiv:2103.15670*, 2021. 8, 11
- [39] Karen Simonyan and Andrew Zisserman. Very deep convolutional networks for large-scale image recognition. *arXiv preprint arXiv:1409.1556*, 2014. 5
- [40] Naman Deep Singh, Francesco Croce, and Matthias Hein. Revisiting adversarial training for imagenet: Architectures, training and generalization across threat models. *Advances in Neural Information Processing Systems*, 36:13931–13955, 2023. 8
- [41] Lukas Struppek, Dominik Hintersdorf, Antonio De Almeida Correia, Antonia Adler, and Kristian Kersting. Plug & play attacks: Towards robust and flexible model inversion attacks. *arXiv preprint arXiv:2201.12179*, 2022. 3, 4, 5, 6, 8, 12, 13, 14, 15, 16, 17
- [42] Lukas Struppek, Dominik Hintersdorf, and Kristian Kersting. Be careful what you smooth for: Label smoothing can be a privacy shield but also a catalyst for model inversion attacks. *arXiv preprint arXiv:2310.06549*, 2023. 1, 3, 4, 12, 13, 16
- [43] Christian Szegedy, Wojciech Zaremba, Ilya Sutskever, Joan Bruna, Dumitru Erhan, Ian Goodfellow, and Rob Fergus. Intriguing properties of neural networks. *arXiv preprint arXiv:1312.6199*, 2013. 6
- [44] Christian Szegedy, Vincent Vanhoucke, Sergey Ioffe, Jon Shlens, and Zbigniew Wojna. Rethinking the inception architecture for computer vision. In *Proceedings of the IEEE conference on computer vision and pattern recognition*, pages 2818–2826, 2016. 5, 12, 13
- [45] Sanli Tang, Xiaolin Huang, Mingjian Chen, Chengjin Sun, and Jie Yang. Adversarial attack type i: Cheat classifiers by significant changes. *IEEE transactions on pattern analysis and machine intelligence*, 43(3):1100–1109, 2019. 1, 2, 3, 4, 6, 7, 8, 9
- [46] Zhengzhong Tu, Hossein Talebi, Han Zhang, Feng Yang, Peyman Milanfar, Alan Bovik, and Yinxiao Li. Maxvit: Multi-axis vision transformer. In *European conference on computer vision*, pages 459–479. Springer, 2022. 5, 8, 12, 13, 15, 17
- [47] Kuan-Chieh Wang, Yan Fu, Ke Li, Ashish Khisti, Richard Zemel, and Alireza Makhzani. Variational model inversion attacks. *Advances in Neural Information Processing Systems*, 34:9706–9719, 2021. 1, 3
- [48] Tianhao Wang, Yuheng Zhang, and Ruoxi Jia. Improving robustness to model inversion attacks via mutual information regularization. In *Proceedings of the AAAI Conference on Artificial Intelligence*, pages 11666–11673, 2021. 1, 3



- [49] Hongxin Wei, Renchunzi Xie, Hao Cheng, Lei Feng, Bo An, and Yixuan Li. Mitigating neural network overconfidence with logit normalization. In *International conference on machine learning*, pages 23631–23644. PMLR, 2022. 7
- [50] Jiawei Yang, Hanbo Chen, Jiangpeng Yan, Xiaoyu Chen, and Jianhua Yao. Towards better understanding and better generalization of few-shot classification in histology images with contrastive learning. 2022. 1
- [51] Ziqi Yang, Jiye Zhang, Ee-Chien Chang, and Zhenkai Liang. Neural network inversion in adversarial setting via background knowledge alignment. In *Proceedings of the 2019 ACM SIGSAC Conference on Computer and Communications Security*, pages 225–240, 2019. 3
- [52] Xiaojian Yuan, Kejiang Chen, Jie Zhang, Weiming Zhang, Nenghai Yu, and Yang Zhang. Pseudo label-guided model inversion attack via conditional generative adversarial network. *Thirty Seventh AAAI Conference on Artificial Intelligence (AAAI 23)*, 2023. 1, 3, 4, 5, 6, 8, 16
- [53] Yuheng Zhang, Ruoxi Jia, Hengzhi Pei, Wenxiao Wang, Bo Li, and Dawn Song. The secret revealer: Generative model-inversion attacks against deep neural networks. In *Proceedings of the IEEE/CVF Conference on Computer Vision and Pattern Recognition*, pages 253–261, 2020. 1, 2, 3, 13, 16, 17

## Supplementary Overview

In this Supp., we provide the code, dataset, additional analysis, detailed experimental reproducibility, discussion on limitation, ethical consideration, and additional visualization of false positives. These sections are not included in the main paper due to space constraints.

- The PyTorch code is included in the submitted Supp. material (i.e., *source-code* folder)
- A portion of the dataset is included in the submitted Supp. material (i.e., *MI-evaluation-dataset* folder). We are unable to submit the entire dataset, as the Supp. material has a file size limit of 200 MB.

## Contents

<b>1. Introduction</b>	<b>1</b>
<b>2. Related Work</b>	<b>3</b>
<b>3. Common Model Inversion (MI) Evaluation Framework <math>\mathcal{F}_{\text{Curr}}</math> has issues</b>	<b>4</b>
3.1. Human-annotated dataset of MI attack samples	4
3.2. What is the issue with the evaluation framework $\mathcal{F}_{\text{Curr}}$ for computing MI AttAcc? . . .	6
<b>4. Significant False Positives by <math>\mathcal{F}_{\text{Curr}}</math> are Type I Adversarial Examples</b>	<b>6</b>
4.1. Adversarial Attack. . . . .	6
4.2. The effect of Type I adversarial features on MI in producing false positives. . . . .	7

4.3. MI Attacks and Type I Adversarial Attacks. .	7
4.4. Our efforts to mitigate the impact of Type I Adversarial Attacks on MI Evaluation . . . .	8
<b>5. Conclusion</b>	<b>8</b>
<b>6. Additional Analysis on MI Evaluation Framework</b>	<b>11</b>
6.1. Discussion on using ViT-based Architecture as Evaluation Models . . . . .	11
6.2. Re-evaluation of MI defenses with human annotated dataset . . . . .	12
<b>7. Additional visualization of false positives</b>	<b>13</b>
<b>8. Detailed experimental reproducibility</b>	<b>13</b>
8.1. Detailed MI setup . . . . .	13
8.2. Computing resources . . . . .	17
<b>9. Limitation</b>	<b>17</b>
<b>10 Ethical consideration</b>	<b>17</b>

## 6. Additional Analysis on MI Evaluation Framework

### 6.1. Discussion on using ViT-based Architecture as Evaluation Models

In the main manuscript, we present the results of using a ViT-based architecture, MaxViT, in  $\mathcal{F}_{\text{Curr}}$  framework. Our results show that replacing the original InceptionNetV3 with MaxViT as  $E$  reduces false positive (FP) rates. In this Supp., we provide a further discussion of these observations. All experimental results in this setup can be found in 6.5.

Generating transferable adversarial examples for ViTs is notably challenging due to their superior robustness [38]. Furthermore, transferring adversarial examples across ViTs and CNNs is even more difficult because their structures and image-processing mechanisms are fundamentally different [26]. Particularly for MI setting, adversarial examples generated by  $T$  are harder to transfer successfully to  $E$  when  $T$  and  $E$  are based on heterogeneous architectures (e.g., CNN and ViT), resulting in lower FP rates.

This argument is supported by the results in Tab. 6.5 in the main manuscript. Across all setups, FP rates consistently decrease when  $T$  and  $E$  are heterogeneous (i.e., one CNN-based and the other ViT-based) compared to when they are homogeneous (i.e., both CNN-based). For example, under the PPA attack with  $T = \text{ResNet18}$ , replacing  $E$  from InceptionNetV3 to MaxViT reduces FP rates by 12.03%.

However, while using a ViT-based architecture as  $E$  reduces FP rates, they remain high. This suggests that the

MI Attack	$\mathcal{D}_{priv}$	$\mathcal{D}_{pub}$	$T$	$\mathcal{F}_{Human}$	$\mathcal{F}_{Curr}$					
				AttAcc $\uparrow$	$E$	AttAcc $\uparrow$	FP rate $\downarrow$	FN rate $\downarrow$	TP rate $\uparrow$	TN rate $\uparrow$
PPA [41]	FaceScrub [29]	FFHQ [20]	ResNet18 [15]	67.50%	InceptionNetV3 [44]	91.39%	89.04%	7.45%	92.52%	10.96%
					MaxViT [46]	79.36%	73.95%	18.03%	81.97%	26.05%
			ResNet101 [15]	74.34%	InceptionNetV3 [44]	84.69%	82.90%	14.69%	85.31%	17.10%
					MaxViT [46]	77.24%	73.25%	21.38%	78.34%	26.75%
			ResNet152 [15]	75.36%	InceptionNetV3 [44]	86.47%	85.87%	13.34%	86.66%	14.13%
					MaxViT [46]	79.61%	77.96%	19.86%	80.14%	22.04%
			DenseNet121 [17]	73.52%	InceptionNetV3 [44]	72.41%	66.52%	25.47%	74.53%	33.48%
					MaxViT [46]	73.51%	58.77%	32.69%	67.31%	41.23%
			MaxViT [46]	70.80%	InceptionNetV3 [44]	79.48%	76.17%	19.15%	80.85%	23.83%
					MaxViT [46]	90.24%	88.85%	9.19%	90.81%	11.15%
IFGMI [35]	FaceScrub [29]	FFHQ [20]	ResNet18 [15]	76.88%	InceptionNetV3 [44]	95.62%	93.72%	3.81%	96.19%	6.28%
					MaxViT [46]	89.01%	85.13%	9.82%	90.18%	14.87%
		MetFaces [21]	ResNet18 [15]	62.14%	InceptionNetV3 [44]	72.13%	69.27%	26.13%	73.87%	30.73%
					MaxViT [46]	59.16%	56.80%	39.41%	60.59%	43.20%

Table 6.5. **Our investigation on the effect of architecture of  $E$  on MI evaluation.** We utilize the advanced and more robust ViT-based architectures MaxViT [46] as  $E$ . In general, with  $E$ =MaxViT, the FP rates is reduced and AttAcc computed by  $\mathcal{F}_{Curr}$  are getting closer to the actual AttAcc. However, the FP rates consistently remain very high suggesting that our findings is architecture-agnostic and driven by Type I adversarial attack influences.

primary issue of FP rates in  $\mathcal{F}_{Curr}$  observed in our comprehensive study is architecture-agnostic and driven by the influences of Type I adversarial attacks.

## 6.2. Re-evaluation of MI defenses with human annotated dataset

Our main focus in this work is MI attacks, where we highlight that the previously reported success rates using the  $\mathcal{F}_{Curr}$  are problematic. In fact, the threat of MI attacks has been overestimated, and the amount of leaked information is considerably less than previously assumed. As recent MI defenses also use  $\mathcal{F}_{Curr}$  to compute MI success rates, we aim to assess the effectiveness of these defenses using our human-annotated dataset.

In this section, we focus on high-resolution setups with PPA. Specifically, we include the latest SOTA MI defenses, such as RoLSS [22], TL [16], LS [42], and TTS [22]. The MI setups strictly follow the configurations in these MI defense studies. The results can be found in Tab. 6.6.

Overall, similar to our observations on MI attacks in the main manuscript,  $\mathcal{F}_{Curr}$  may inaccurately assess the effectiveness of SOTA MI defenses. For example, we observe a mismatch between AttAcc comparisons via  $\mathcal{F}_{Curr}$  and actual AttAcc measured by  $\mathcal{F}_{Human}$ . For example, AttAcc

via  $\mathcal{F}_{Curr}$  suggests that LS [41] and TL [16] outperform RoLSS and TTS [22]. However, actual AttAcc indicates that RoLSS and TTS are more effective defenses. In what follows, we further discuss these results.

These MI defenses result in reduction of FP rates due to degrading the transferability of adversarial features from  $T$  to  $E$ . Specifically, *Under TL defense [16]*, only the later layers of  $T$  are fine-tuned on  $\mathcal{D}_{priv}$ , while earlier layers are frozen from the pre-trained backbone. Hence, later layers of  $T$  captures  $\mathcal{D}_{priv}$  features, while earlier layers of  $T$  captures  $\mathcal{D}_{pretrain}$  features. In contrast,  $E$  captures  $\mathcal{D}_{priv}$  features across all layers since all layers of  $E$  are fine-tuned on  $\mathcal{D}_{priv}$ . This mismatch in feature representations between  $T$  and  $E$  under TL likely reduces adversarial transferability [? ? ], thereby reducing FP rates. Under LS defense [42], negative label smoothing (LS) is employed to improve MI robustness. LS slightly reduces label dominance and weakens gradient alignment between surrogate and target models [? ]. Negative LS amplifies this effect, further degrading gradient similarity. Therefore, training  $T$  with negative LS diminishes gradient alignment with  $E$  (trained on standard labels), reducing adversarial transferability [? ? ]. Under RoLSS and TTS defenses [22], removing certain skip connections improves resilience to MI attacks. Skip con-

MI Attack	$\mathcal{D}_{priv}$	$\mathcal{D}_{pub}$	$T$ / MI Defense	Natural Acc $\uparrow$	$\mathcal{F}_{Human}$	$E$	$\mathcal{F}_{Curr}$				
					AttAcc $\downarrow$		AttAcc $\downarrow$	FP rate $\uparrow$	FN rate $\uparrow$	TP rate $\downarrow$	TN rate $\downarrow$
PPA [41]	FaceScrub [29]	FFHQ [20]	ResNet101 / No Defense [15]	94.86%	74.34%	InceptionNetV3 [44]	84.69%	82.90%	14.69%	85.31%	17.10%
			ResNet101 / RoLSS [22]	92.98%	57.54%		43.39%	42.77%	56.15%	43.85%	57.23%
			ResNet101 / TL [16]	92.51%	74.91%		34.17%	31.02%	64.77%	35.23%	68.98%
			ResNet101 / TTS [22]	94.16%	64.20%		42.52%	39.53%	55.80%	44.20%	60.47%
			ResNet101 / LS [42]	92.21%	62.92%		16.56%	14.12%	82.01%	17.99%	85.88%

Table 6.6. **Our investigation on the effectiveness of MI defenses using our human-annotated dataset of MI attack samples.** We present the results of the latest MI defenses including RoLSS [22], TL [16], LS [42], and TTS [22]. We observe a mismatch between AttAcc comparisons via  $\mathcal{F}_{Curr}$  and actual AttAcc measured by  $\mathcal{F}_{Human}$ . Overall, consistent with our findings on MI attacks, this suggests that  $\mathcal{F}_{Curr}$  may have issues in evaluating MI defenses.

nections are known to improve adversarial transferability [?]. By modifying  $T$  to remove some skip connections, adversarial examples generated by  $T$  transfer less effectively to  $E$ .

Regarding FN rates, although this is not the main focus of our study, we observe that FN rates tend to increase under MI defenses compared to MI attacks. FN rates depend on the classification accuracy and generalization capability of  $E$ . SOTA MI defenses introduce various strategies (e.g., fixing earlier layers trained on public data [16], perturbing labels [42], and removing skip connections [22]) to encode less information in the predictions of  $T$ . These approaches may encourage  $T$  to learn more generalized features. As a result, reconstructed images based on these generalized features of  $T$  may differ more from the seen training data. However, in the prevalent MI setups,  $E$  in  $\mathcal{F}_{Curr}$  is often trained with standard training procedures and architectures. This could limit its generalization capacity, making it less capable of accurately classifying these reconstructed images via the target models  $T$  under MI defenses.

## 7. Additional visualization of false positives

In the main manuscript, we provide some visualizations of MI false positives. In this Supp., we provide more extensive visualizations of MI false positives in Fig. 7.3, 7.4, 7.5, 7.6, 7.7, 7.8, 7.9, 7.10, 7.11, 7.12, 7.13.

These MI false positives do not capture visual identity features of the target individual in the private training data, but they are still deemed successful attacks according to  $\mathcal{F}_{Curr}$  with a high confidence.

## 8. Detailed experimental reproducibility

### 8.1. Detailed MI setup

To ensure the reproducibility, we strictly follow previous studies [5, 16, 22, 31, 35, 41, 53] for MI setups.

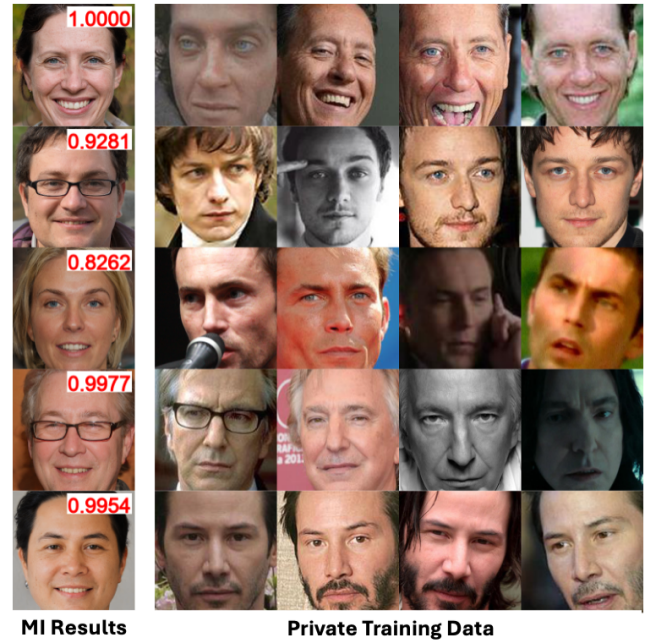


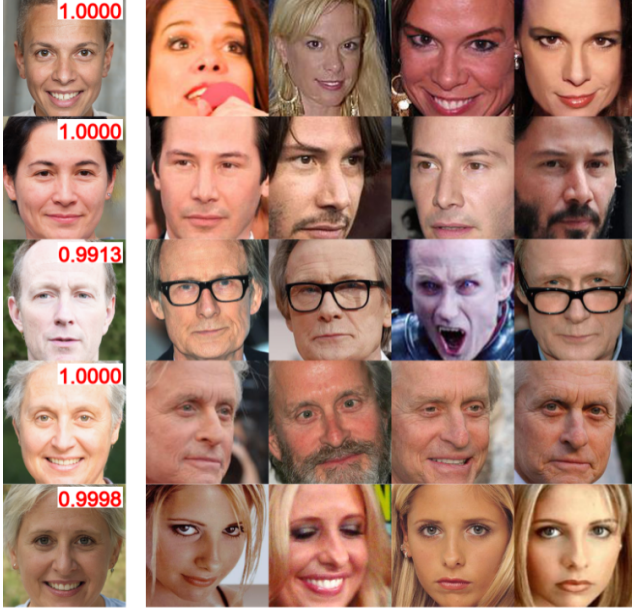
Figure 7.3. Additional visualization of false positives. These MI false positives do not capture visual identity features of the target individual in the private training data, but they are still deemed successful attacks according to  $\mathcal{F}_{Curr}$  with a high confidence (indicated in red text). Here,  $T$ =MaxViT [46],  $\mathcal{D}_{priv}$ =FaceScrub [29],  $\mathcal{D}_{pub}$ =FFHQ [20],  $E$ =InceptionNetV3 under PPA attack [41].

**MI attacks.** Our study focuses on SOTA GAN-based MI attack that achieve strong performance in computer vision domain. These attacks optimize the GAN latent space rather than directly optimize the image space.

*KEDMI* [5] Introduces an MI-specific GAN that incorporates knowledge from the target classifier. The discriminator performs dual tasks: distinguishing real and fake samples and predicting class-wise labels.

*LOMMA* [31] Improves MI attacks using a novel logit

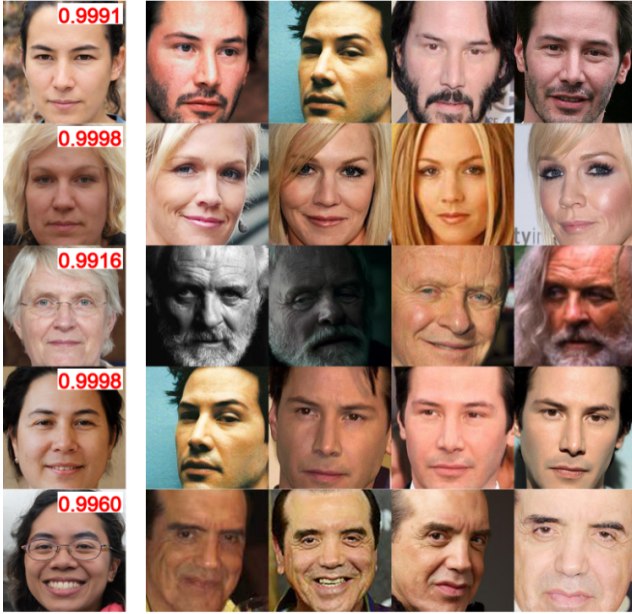




**MI Results**

**Private Training Data**

Figure 7.4. Additional visualization of false positives. These MI false positives do not capture visual identity features of the target individual in the private training data, but they are still deemed successful attacks according to  $\mathcal{F}_{Curr}$  with a high confidence (indicated in red text). Here,  $T$ =DenseNet121,  $\mathcal{D}_{priv}$ =FaceScrub,  $\mathcal{D}_{pub}$ =FFHQ,  $E$ =InceptionNetV3 under PPA attack.



**MI Results**

**Private Training Data**

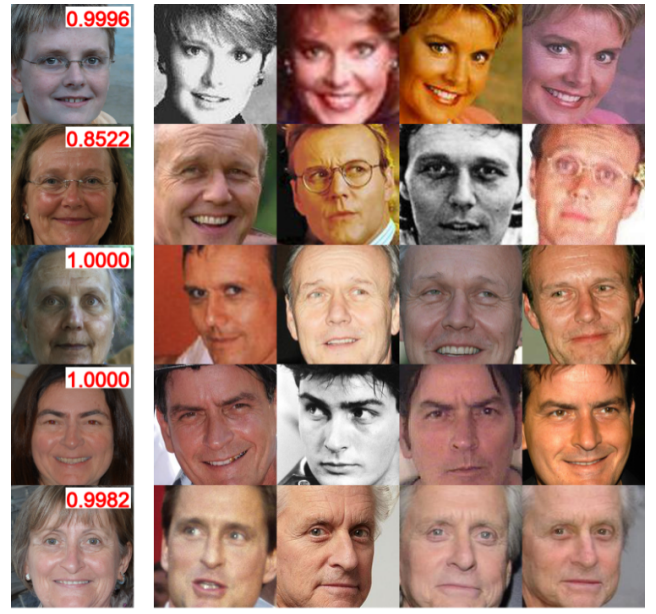
Figure 7.5. Additional visualization of false positives. These MI false positives do not capture visual identity features of the target individual in the private training data, but they are still deemed successful attacks according to  $\mathcal{F}_{Curr}$  with a high confidence (indicated in red text). Here,  $T$ =ResNet101 [15],  $\mathcal{D}_{priv}$ =FaceScrub [29],  $\mathcal{D}_{pub}$ =FFHQ [20],  $E$ =InceptionNetV3 under PPA attack [41].



**MI Results**

**Private Training Data**

Figure 7.6. Additional visualization of false positives. These MI false positives do not capture visual identity features of the target individual in the private training data, but they are still deemed successful attacks according to  $\mathcal{F}_{Curr}$  with a high confidence (indicated in red text). Here,  $T$ =ResNet152 [15],  $\mathcal{D}_{priv}$ =FaceScrub [29],  $\mathcal{D}_{pub}$ =FFHQ [20],  $E$ =InceptionNetV3 under PPA attack [41].



**MI Results**

**Private Training Data**

Figure 7.7. Additional visualization of false positives. These MI false positives do not capture visual identity features of the target individual in the private training data, but they are still deemed successful attacks according to  $\mathcal{F}_{Curr}$  with a high confidence (indicated in red text). Here,  $T$ =ResNet18,  $\mathcal{D}_{priv}$ =FaceScrub,  $\mathcal{D}_{pub}$ =FFHQ,  $E$ =InceptionNetV3 under IFGMI attack.

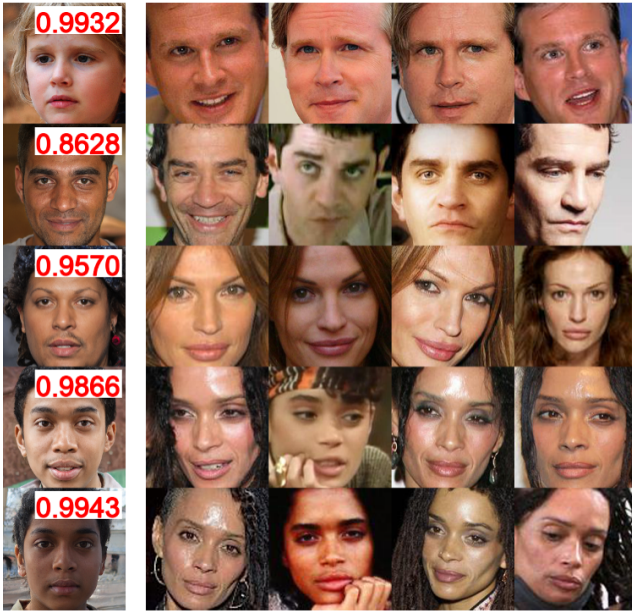




**MI Results**

**Private Training Data**

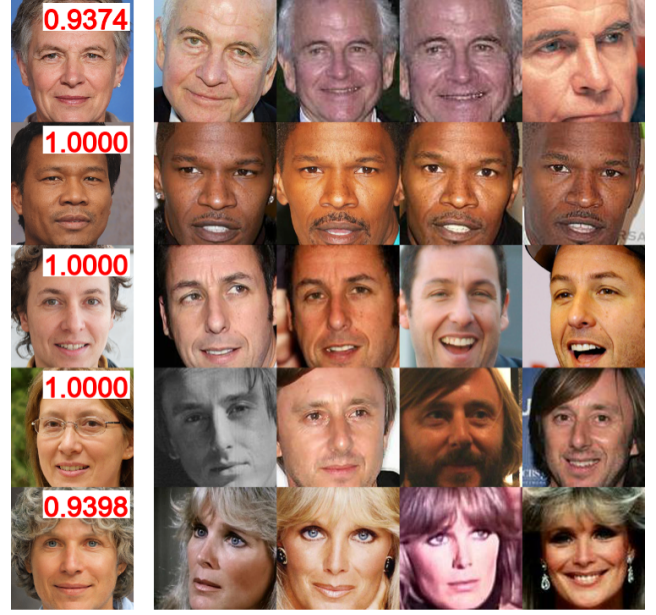
Figure 7.8. Additional visualization of false positives. These MI false positives do not capture visual identity features of the target individual in the private training data, but they are still deemed successful attacks according to  $\mathcal{F}_{Curr}$  with a high confidence (indicated in red text). Here,  $T$ =ResNet18 [15],  $\mathcal{D}_{priv}$ =FaceScrub [29],  $\mathcal{D}_{pub}$ =FFHQ [20],  $E$ =MaxViT under IFGMI attack [35].



**MI Results**

**Private Training Data**

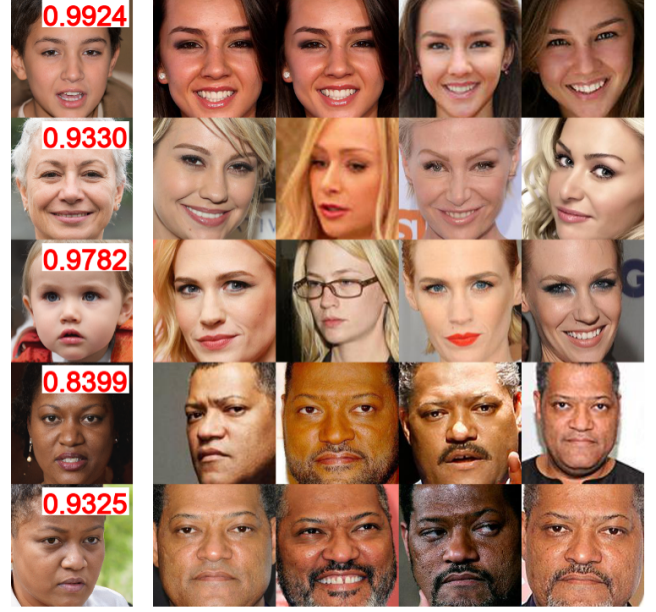
Figure 7.9. Additional visualization of false positives. These MI false positives do not capture visual identity features of the target individual in the private training data, but they are still deemed successful attacks according to  $\mathcal{F}_{Curr}$  with a high confidence (indicated in red text). Here,  $T$ =DenseNet121,  $\mathcal{D}_{priv}$ =FaceScrub,  $\mathcal{D}_{pub}$ =FFHQ,  $E$ =MaxViT under PPA attack.



**MI Results**

**Private Training Data**

Figure 7.10. Additional visualization of false positives. These MI false positives do not capture visual identity features of the target individual in the private training data, but they are still deemed successful attacks according to  $\mathcal{F}_{Curr}$  with a high confidence (indicated in red text). Here,  $T$ =MaxViT [46],  $\mathcal{D}_{priv}$ =FaceScrub [29],  $\mathcal{D}_{pub}$ =FFHQ [20],  $E$ =MaxViT under PPA attack [41].

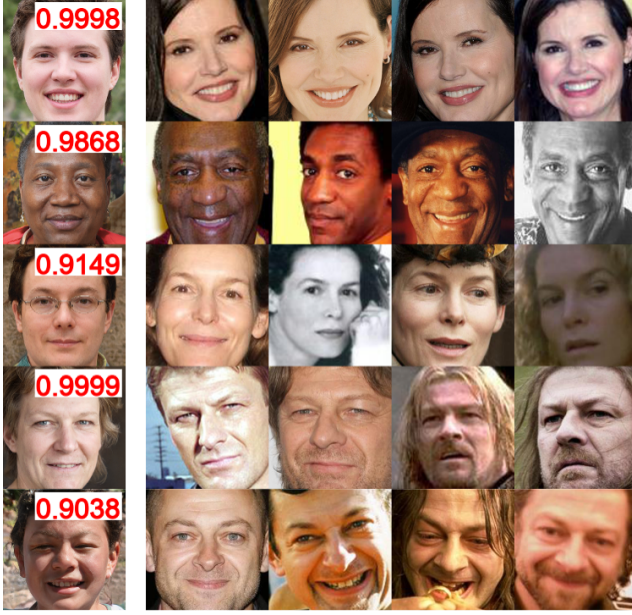


**MI Results**

**Private Training Data**

Figure 7.11. Additional visualization of false positives. These MI false positives do not capture visual identity features of the target individual in the private training data, but they are still deemed successful attacks according to  $\mathcal{F}_{Curr}$  with a high confidence (indicated in red text). Here,  $T$ =ResNet18 [15],  $\mathcal{D}_{priv}$ =FaceScrub [29],  $\mathcal{D}_{pub}$ =FFHQ [20],  $E$ =MaxViT under PPA attack [41].





**MI Results**

**Private Training Data**

Figure 7.12. Additional visualization of false positives. These MI false positives do not capture visual identity features of the target individual in the private training data, but they are still deemed successful attacks according to  $\mathcal{F}_{Curr}$  with a high confidence (indicated in red text). Here,  $T$ =ResNet101 [15],  $\mathcal{D}_{priv}$ =FaceScrub [29],  $\mathcal{D}_{pub}$ =FFHQ [20],  $E$ =MaxViT under PPA attack [41].



**MI Results**

**Private Training Data**

Figure 7.13. Additional visualization of false positives. These MI false positives do not capture visual identity features of the target individual in the private training data, but they are still deemed successful attacks according to  $\mathcal{F}_{Curr}$  with a high confidence (indicated in red text). Here,  $T$ =ResNet152 [15],  $\mathcal{D}_{priv}$ =FaceScrub [29],  $\mathcal{D}_{pub}$ =FFHQ [20],  $E$ =MaxViT under PPA attack [41].

loss and model augmentation to mitigate overfitting.

**PLGMI** [52] Leverages conditional GANs to isolate class-specific search spaces and uses Max-Margin Loss to address vanishing gradients in MI optimization.

**PPA** [41] Utilizes powerful StyleGAN for high-resolution image MI attacks, emphasizing a modular design adaptable to different architectures and datasets.

**IFGMI** [35] Proposes Intermediate Features Generative Model Inversion, extending optimization from latent codes to intermediate features, enhancing the attack’s expressive capability.

**MI defense.** Our study focuses on SOTA MI defenses. Differ from MI attacks, MI defenses aim to minimize the disclosure of training samples during the MI optimization process.

**TL** [16] Leverages Transfer Learning to limit sensitive information encoding in earlier layers, degrading MI attack performance.

**LS** [42] Introduces label smoothing with negative factors to impede class-related information extraction.

**RoLSS** [22] Demonstrates that removing skip connections in the last stage significantly reduces MI attack accuracy, offering a better MI robustness trade-off.

**TTS** [22] Building on top of RoLSS. Particularly, in the first stage, the model  $T$  with full skip-connections archi-

itecture is trained on private dataset. Then in the stage 2, the skip connection removed architecture, i.e. RoLSS, is fine-tuned on private dataset. The pre-trained parameters in Stage 1 serves as initialization for the stage 2, thereby improve the convergence of model in stage 2.

**Private training data  $\mathcal{D}_{priv}$ .** Following previous works [5, 16, 22, 31, 35, 41, 53], we focus on reconstruction of images and use the face recognition as a running example including FaceScrub [29] and CelebA [25].

**FaceScrub** [29]: FaceScrub provides cropped facial images for 530 identities. The dataset publicly a total of 37,878 images. After train/test splitting, this resulted in 34,090 training samples and 3,788 test samples.

**CelebA** [25]: CelebA is a dataset of celebrity facial images available for non-commercial research. Following previous works [5, 16, 22, 31, 35, 41, 53], we select the top 1,000 identities with the most samples from 10,177 available identities, resulting in 27,034 training samples and 3,004 test samples.

**Public data for GAN  $\mathcal{D}_{pub}$ .** Following the data preparation in previous works [5, 16, 22, 31, 35, 41, 53], we use  $\mathcal{D}_{pub}$  ensuring that the dataset  $\mathcal{D}_{priv}$  and  $\mathcal{D}_{pub}$  with no class intersection.  $\mathcal{D}_{priv}$  is used to train the target classifier  $T$ ,



while  $\mathcal{D}_{pub}$  is used to train GAN to extract general features only.

*CelebA* [25]: Following previous works [5, 16, 31, 53], we select 30,000 images from identities distinct from the 1,000 identities in  $\mathcal{D}_{priv}$ .

*FFHQ* [25]: This dataset contains 70,000 high-quality human face images sourced from Flickr, offering significant diversity in age, ethnicity, and backgrounds.

*MetFaces* [20]. This dataset includes 1,336 high-quality artistic renderings of human faces, covering various art styles. The images exhibit significant diversity and uniqueness.

**Target Classifier  $T$ .** Following previous works [5, 16, 22, 31, 35, 41, 53], we include a wide ranges of architectures as  $T$  in our study including ResNet18/101/152 [15], DenseNet121[17], MaxViT [46], FaceNet [5], and VGG16 [15]. To ensure the reproducibility, we utilize the checkpoints of these target classifier in the previous works.

## 8.2. Computing resources

We conducted all experiments on NVIDIA RTX A5000 GPUs running Ubuntu 20.04.2 LTS, with AMD Ryzen Threadripper PRO 5975WX 32-Core processors. The environment setup includes CUDA 12.2, Python 3.8.18, and PyTorch 1.12.0 with Torchvision 0.14.1. For high-resolution tasks, [35, 41], we use model architectures and pre-trained ImageNet backbone weights from Torchvision. For the low-resolution setup, following [5, 16, 31], we employed VGG architecture with pre-trained ImageNet weights from Torchvision, while we utilize IR152 and FaceNet architectures with pre-trained backbones from face.evoLve<sup>1</sup>.

## 9. Limitation

While this study provides valuable insights into the limitations of the MI evaluation framework and establishes a comprehensive human-annotated dataset for future study, it is important to acknowledge certain limitations. One such limitation is the focus on specific architectures and datasets. While we strictly follow previous works [5, 16, 22, 31, 35, 41, 53] to includes 28 MI setups (spanning 3 evaluation model, 9 target classifier, 2 private dataset, 3 public dataset), these setups may not include the latest architectures or dataset that are not considered in prevalent MI setups. Future research could expand upon our findings by exploring a wider range of model architectures and datasets. This would further shed the light of MI evaluation and contribute to the development of better MI evaluation frameworks.

---

<sup>1</sup><https://github.com/ZhaoJ9014/face.evoLve>

## 10. Ethical consideration

This study examines the limitations of widely used evaluation frameworks for Model Inversion (MI) attacks, which hold critical implications for privacy and data security. We construct a comprehensive human-annotated dataset using anonymous user voting, ensuring no personal information is collected. Analysis of this dataset reveals an overestimation of MI attack success rates, underscoring the need for accurate and reliable evaluation metrics to avoid inflated perceptions of privacy risks. To support the research community, we release the dataset and code, advocating for their ethical use to advance privacy protection. Additionally, we urge further research into improved and reliable automatic evaluation frameworks.